On the Nature of the "Bleaching out" Process of the ^{35}Cl NQR Signals in 1,2,3-Trichlorobenzene *

Silvia Wigand **, Norbert Weiden, and Alarich Weiss

Institut für Physikalische Chemie, Physikalische Chemie III, Technische Hochschule Darmstadt,
Darmstadt, West Germany

Z. Naturforsch. **45 a**, 490–502 (1990); received October 9, 1989

The ^{35}Cl NQR frequencies, linewidths, and spin-lattice relaxation times $T_1(^{35}\text{Cl})$ of 1,2,3-trichlorotrideuterobenzene were measured at various temperatures. The deuterated compound shows the same bleaching out phenomenon as 1,2,3-trichlorobenzene. Single crystal ^{2}H NMR measurements were carried out at 295 and 193 K. The nuclear quadrupole coupling constants at room temperature are in the range of $175.8 \leqq e^2qQh^{-1}(^2\text{H})/\text{kHz} \leqq 179.5$, and the asymmetry parameters η in the range of $0.060 \leqq \eta(^2\text{H}) \leqq 0.073$. As for the principal axes of the electric field gradient tensor, it was found that $\Phi_{zz}(^2\text{H})$ is parallel to the C–D bond, $\Phi_{yy}(^2\text{H})$ is perpendicular to the benzene ring plane and $\Phi_{xx}(^2\text{H})$ lies in the ring plane. The linewidths of the ^{2}H NMR satellites are idependent of temperature. For the undeuterated compound, the temperature dependence of $T_1(^1\text{H})$ was also measured. The mechanism leading to the bleaching out of the ^{35}Cl NQR signals is discussed.

Introduction

Several processes in the solid state can lead to a broadening and final disappearance of ^{35}Cl NQR frequencies far below the melting point. This phenomenon, termed "bleaching out", is observed for many compounds and can be interpreted by

1) the formation of disorder in the crystal structure, as observed for some di- and hexasubstituted halogenobenzenes [1, 2],
2) reorientational motions,
3) the formation and migration of lattice vacancies [3].

The bleaching out process is also observed for 1,2,3-trichlorobenzene, 1,2,3-$Cl_3H_3C_6$, and the mechanism is still under discussion [4, 5, 6].

The crystal structure of this compound was determined at room temperature by neutron diffraction by Hazell et al. [7]. 1,2,3-$Cl_3H_3C_6$ crystallizes with the monoclinic space group C_{2h}^5–P2_1/c. With $Z=8$, the asymmetric unit of the cell contains 2 molecules. In Fig. 1, a projection of the crystal structure (taken from [6]) along the ***b*** axis onto the ***a***, ***c*** plane is shown. In agreement with the structure, six ^{35}Cl NQR signals are observed at $T=77$ K. No signals, however, are detectable at room temperature [8, 9].

Based on the observed temperature dependence of the linewidths $\Delta\nu$ of the ^{35}Cl NQR and ^{1}H NMR signals and the dielectric constant of 1,2,3-$Cl_3H_3C_6$, Tatsuzaki proposed a reorientational motion of the molecules around an axis normal to the ring plane [4]. Such a motion was concluded from the temperature dependence of the dielectric constant for several hexa-substituted benzene derivatives by White et al. [10].

Sharma et al. studied the six ^{35}Cl nuclear quadrupole coupling tensors by single crystal Zeeman split NQR and assigned the $\nu_i(^{35}\text{Cl})$ to the corresponding Cl atoms. Measurements of $\nu=f(T)$ and $\Delta\nu=f(T)$ show that the ^{35}Cl NQR signals die out in the range $225 \leqq T/\text{K} \leqq 255$ [6]. Interestingly the signals of molecule I broaden and die out at lower temperature than those of molecule II. From the temperature dependence of the spin-lattice relaxation time $T_1(^{35}\text{Cl})$, an activation energy E_A for the bleaching out process was calculated: $E_A \approx 30$ kJ mol^{-1} for molecule I and $E_A \approx 35$ kJ mol^{-1} for molecule II. Furthermore, it was observed that the asymmetry parameter $\eta(^{35}\text{Cl})$ of the electric field gradient (EFG) tensor, which is described by

$$\eta = (|\Phi_{xx} - \Phi_{yy}|)/|\Phi_{zz}| \qquad (1)$$

(where Φ_{xx}, Φ_{yy} and Φ_{zz} are the principal axes of the EFG tensor), does not depend on temperature. For that reason an order-disorder mechanism, which is static in the time scale of ^{35}Cl NQR, was proposed [6].

---

* Presented at the Xth International Symposium on Nuclear Quadrupole Resonance Spectroscopy, Takayama, Japan, August 22–26, 1989.

** Part of Dr.-Ing. Thesis of Silvia Wigand, D 17, Technische Hochschule Darmstadt.

Reprint requests to Prof. Dr. Al. Weiss, Institut für Physikalische Chemie III, Technische Hochschule Darmstadt, Petersenstraße 20, D-6100 Darmstadt.

0932-0784 / 90 / 0300-0490 $ 01.30/0. – Please order a reprint rather than making your own copy.

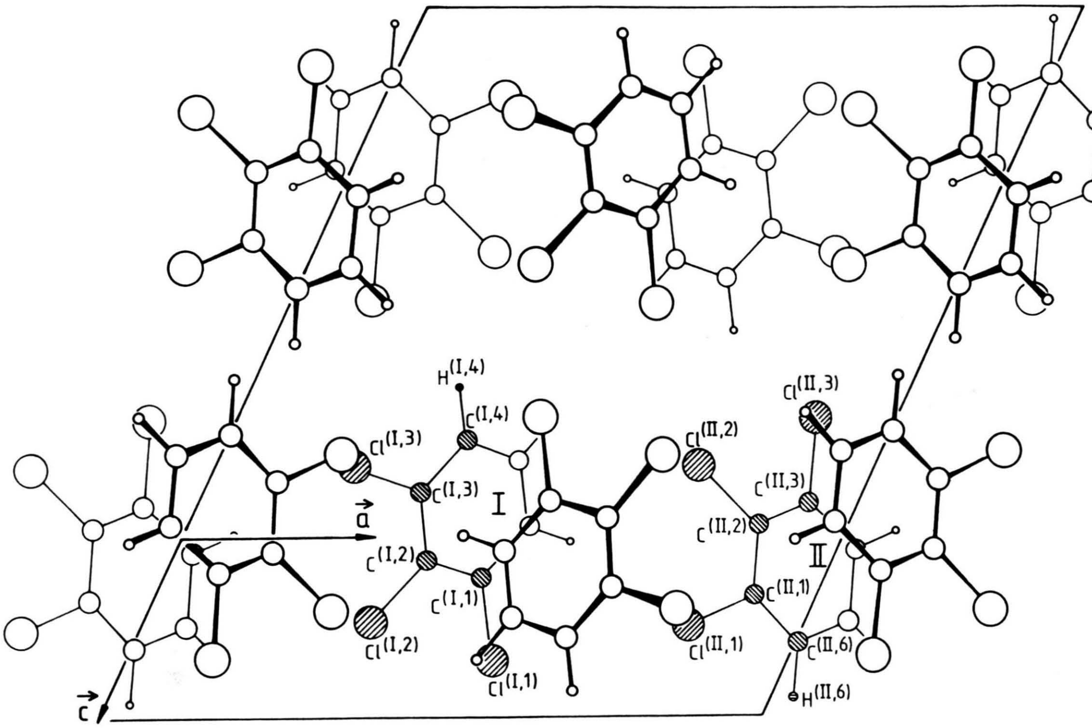

Fig. 1. Projection of the crystal structure of 1,2,3-trichlorobenzene along the ***b*** axis onto the plane ***a***, ***c***. The crystallographically different molecules I and II, for which the positional parameters are listed in [1] are marked by I and II.

To get a deeper insight into the nature of the bleaching out process, we studied the ^{2}H nuclear quadrupole coupling tensors in 1,2,3-$Cl_3D_3C_6$ by high field single crystal ^{2}H NMR. For comparison of the deuterated compound with the undeuterated one, we also measured the temperature dependence of $\nu(^{35}Cl)$, $\Delta\nu(^{35}Cl)$ and $T_1(^{35}Cl)$ of polycrystalline 1,2,3-$Cl_3D_3C_6$.

Experimental

Preparation and Single Crystal Growth

1,2,3-$Cl_3D_3C_6$, was prepared from 1,2,3-$Cl_3H_3C_6$ and D_2O in the presence of a catalyst. Acid-catalyzed hydrogen exchange [11, 12] as well as platinum catalyzed hydrogen exchange [13] was applied. 6–8 g trichlorobenzene and 6–8 ml D_2O/DCl solution, which was recycled from higher exchange cycles, was filled into a glass ampoule. The sealed tube then was transferred into an autoclave, which was heated for 6–7 days at $T = 320$ °C. The deuterium content of the product obtained from the first exchange cycles was in the range of 30%–50% (determined by ^{1}H-NMR). For the following reaction cycles, 10% DCl solution, which was prepared from 99.75% D_2O and 99% DCl, was used. After four exchange cycles, a deuterium content of 80%–90% was obtained. For the last 2–3 cycles, the heterogeneous exchange was applied, using a 5% Pt-coal catalyst [13]. The reaction time was 3 days, $T = 180$ °C. In this way 30 g of highly deuterated 1,2,3-trichlorobenzene was prepared and subsequently purified by zone melting. The melting point was 53 °C.

Large single crystals (1 cm × 1 cm × 0.5 cm) were grown from a saturated solution of the compound in ethanol by slow cooling the seeded solution from 30 °C down to room temperature. They form colourless prisms with faces {001}, {100}, and {111}.

^{35}Cl NQR

^{35}Cl NQR frequencies, linewidths $\Delta\nu$, and spin-lattice relaxation times $T_1(^{35}Cl)$ were measured with a Bruker CXP 200 spectrometer using polycrystalline sample. $T_1(^{35}Cl)$ was determined by the $180°-\tau-90°$ method. The sample was held at constant temperature to ±0.2 K by a heated (cooled) stream of nitrogen gas.

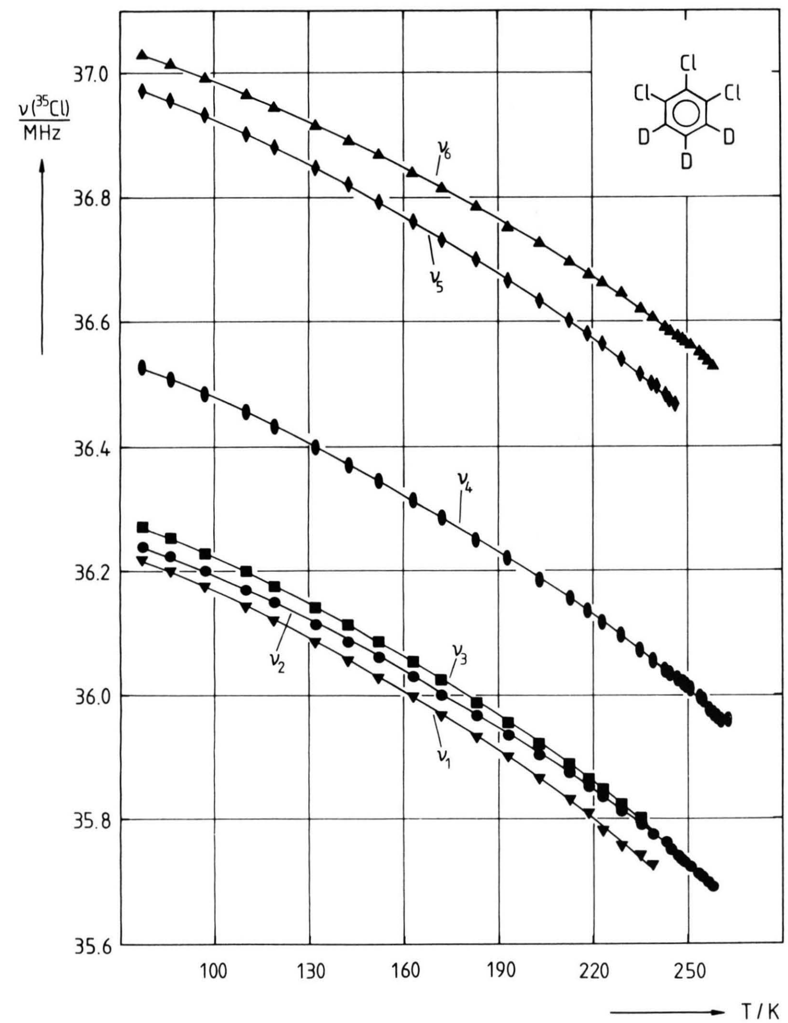

Fig. 2. Temperature dependence of the ^{35}Cl NQR lines of 1,2,3-trichlorotrideuterobenzene. $Cl^{(I,1)}$: ▼; $Cl^{(I,2)}$: ◆; $Cl^{(I,3)}$: ■; $Cl^{(II,1)}$: ●; $Cl^{(II,2)}$: ▲; $Cl^{(II,3)}$: ●.

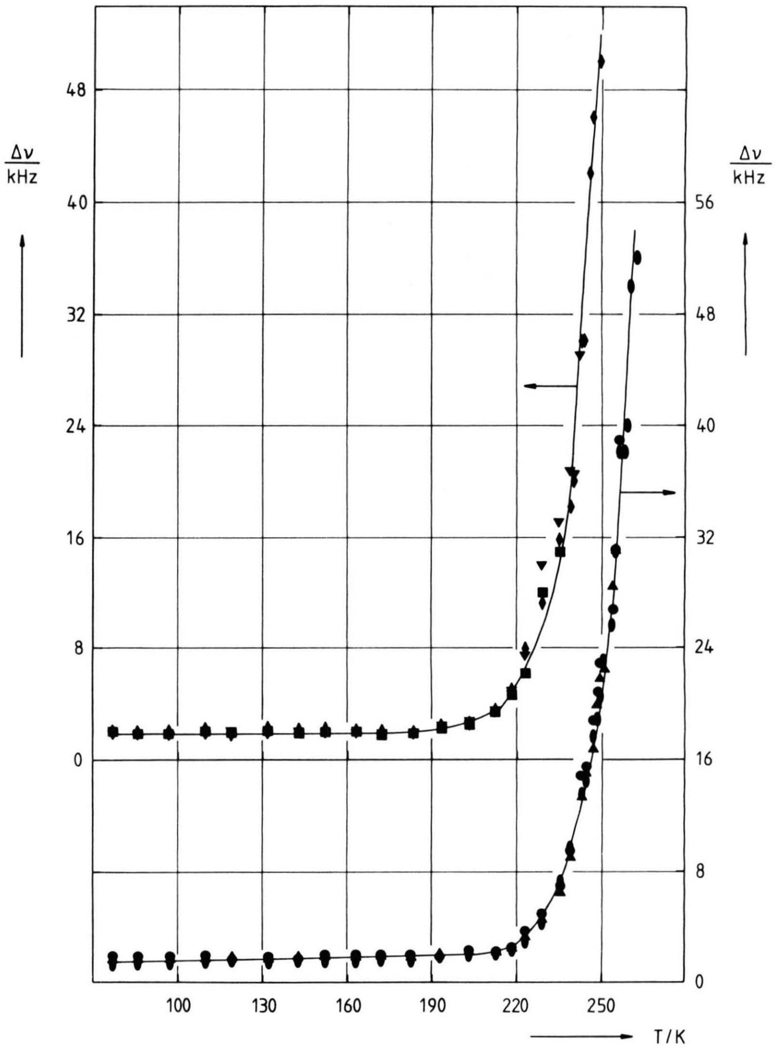

Fig. 3. Width $\Delta\nu$ of the ^{35}Cl NQR lines of 1,2,3-$Cl_3D_3C_6$ vs. temperature. $Cl^{(I,1)}$: ▼; $Cl^{(I,2)}$: ◆; $Cl^{(I,3)}$: ■; $Cl^{(II,1)}$: ●; $Cl^{(II,2)}$: ▲; $Cl^{(II,3)}$: ●.

^{2}H and ^{1}H NMR

The ^{2}H and ^{1}H NMR spectra were measured with the Bruker spectrometer applying a magnetic field of 4.7 T. The Larmor frequency (ν_L) of ^{2}H at this field is 30.720 MHz. At 295 K, crystals of 1,2,3-$Cl_3D_3C_6$ were rotated in the magnetic field about three mutually perpendicular axes, and the spectra were analysed according Volkoff and coworkers [14, 15]. The rotation axes were X, Y, Z [$\sphericalangle(\boldsymbol{a}, X) = \beta - 90°$, $\boldsymbol{b} \parallel Y$, $\boldsymbol{c} \parallel Z$]. At 193 K, the crystal was rotated about the X axis. The temperature dependence of the ^{1}H spin-lattice relaxation time T_1 of polycrystalline 1,2,3-$Cl_3H_3C_6$ was determined using the $180° - \tau - 90°$ method at 4.7 T.

Results

^{35}Cl NQR

The temperature dependence of the ^{35}Cl NQR frequencies of 1,2,3-$Cl_3D_3C_6$ is shown in Figure 2. In Table 1 the coefficients a_n of the equation

$$\nu(^{35}\text{Cl}) = \sum_n a_n T^n \tag{2}$$

are listed. The observed linewidths are shown in Figure 3. Figs. 4a–c show the results of the T_1 (^{35}Cl) measurements. The temperature dependence of the ^{35}Cl NQR frequencies as well as the linewidths and spin-lattice relaxation time T_1 (^{35}Cl) of 1,2,3-$Cl_3D_3C_6$ is the same as for the undeuterated compound investigated by Sharma et al. [6].

^{2}H NMR

The unit cell of 1,2,3-trichlorobenzene contains 24 ^{2}H-atoms [7]. The inversion center reduces the number of NMR-distinguishable atoms to 12; hence, in the general case 12 satellite pairs ($\nu_L + \delta\nu$, $\nu_L - \delta\nu$) are expected. Figures 5 and 6 show the rotation patterns about the X axis [$\sphericalangle(\boldsymbol{a}, X) = \beta - 90°$] and the Z axis ($\boldsymbol{c} \parallel Z$), respectively. Special orientations reduce the number of satellite pairs in the spectrum. EFG tensors which are connected by a mirror plane, m, become equivalent if the magnetic field $\boldsymbol{B}_0$ is parallel to m. When the crystal is rotated about the $\boldsymbol{b}$ axis, m is always parallel to $\boldsymbol{B}_0$. Therefore the rotation pattern consists only of 6 satellite pairs instead of 12 in the general case. In Fig 7, the patterns for rotation about the $\boldsymbol{b}$ axis ($\boldsymbol{b} \parallel Y$) is shown. $\boldsymbol{B}_0$ stays parallel to the mirror plane m for $0 \leqq \varphi/\text{deg} \leqq 180$. The curves in Figs. 5–7 were expressed by functions of the type

$$2\delta\nu = A_i + B_i \cos(2\varphi) + C_i \sin(2\varphi), \tag{3}$$

$i = X, Y, Z$. The resulting constants A_i, B_i, C_i are given in Table 2.

The nuclear quadrupole coupling constants, NQCC, $e^2qQh^{-1}(^2\text{H})$, asymmetry parameters $\eta(^2\text{H})$ and the direction cosines of the principal axes of the ^{2}H EFG tensors of 1,2,3-$Cl_3D_3C_6$ were evaluated by the method of Volkoff and coworkers [14, 15]. Application of the Volkoff analysis leads to an uncertainty in the sign of the coefficients C_z in the coefficient matrix as pointed out by Hutton and Pedersen [16]. In the case 1,2,3-$Cl_3D_3C_6$ one solution leads to η-values in the range of $0.2 \leqq \eta \leqq 0.9$. These values are unrealistic and were rejected. The other solution leads to η-values in the range of $0.06 \leqq \eta \leqq 0.073$ (see Table 3, in which $\eta(^2\text{H})$ and $e^2qQh^{-1}(^2\text{H})$ are given for room temperature), which are typical values for ^{2}H bound to the aromatic ring [17, 18].

The direction cosines of the principal axes Φ_{xx}, Φ_{yy} and Φ_{zz} of the ^{2}H EFG tensors are given in Table 4 together with the direction cosines of the corresponding C–D bond. It should be noted that in [6] a different orthogonal axes system is used, with the monoclinic angle β between the $\boldsymbol{c}$-axis and Z and $\boldsymbol{a} \parallel X$. Here we use the usual setting because then the orthogonal axes X, Y, Z coincide with the rotation axes of the crystal. The orientation of the principal axes with respect to the molecules can be taken from Table 5. Φ_{xx}, Φ_{yy} and Φ_{zz} are handeled as a system of right-handed vectors although $\tilde{\boldsymbol{\Phi}}$ is a second rank tensor. In this way ± signs are avoided. The signs are chosen in such a way, that Φ_{zz} is parallel to the C–D bond.

In Fig. 8, the result of the ^{2}H NMR measurements at low temperature ($T = 193$ K) is shown. The rotation axis was X [$\sphericalangle(\boldsymbol{a}, X) = \beta - 90°$]. The coefficients A_X, B_X and C_X are listed in Table 6. The temperature dependence of the spin-lattice relaxation time T_1 of the protons in polycrystalline 1,2,3-$Cl_3H_3C_6$ is shown in Figure 9. $T_1(^1\text{H})$ at room temperature is ≈ 50 s. With decreasing temperature, $T_1(^1\text{H})$ increases exponentially. The experiment was finished at $T \approx 220$ K because measurements of T_1 in the order of magnitude of hours are tedious and the 5 values are sufficient to evaluate the activation energy.

Table 1. Coefficients of the parametrization of the NQR frequencies $\nu_i(^{35}\mathrm{Cl})$ of 1,2,3-$\mathrm{Cl_3D_3C_6}$ as a function of temperature according to the equation $\nu_i(^{35}\mathrm{Cl}) = f(T) = a_0 + a_{-1}\,T^{-1} + a_1\,T + a_2\,T^2$.

$\nu(^{35}\mathrm{Cl})$	$\dfrac{a_{-1}}{\mathrm{MHz\,K}}$	$\dfrac{a_0}{\mathrm{MHz}}$	$\dfrac{a_1 \cdot 10^4}{\mathrm{MHz\,K^{-1}}}$	$\dfrac{a_2 \cdot 10^6}{\mathrm{MHz\,K^{-2}}}$
ν_1	0.9215	36.3324	−11.7696	−5.6887
ν_2	2.6503	36.3009	− 7.0672	−6.4700
ν_3	−0.4012	36.4096	−12.6749	−5.5629
ν_4	3.5652	36.5664	− 5.4412	−6.9567
ν_5	5.2024	36.9659	− 1.6069	−7.9104
ν_6	5.6998	36.9983	0.5557	−7.5605

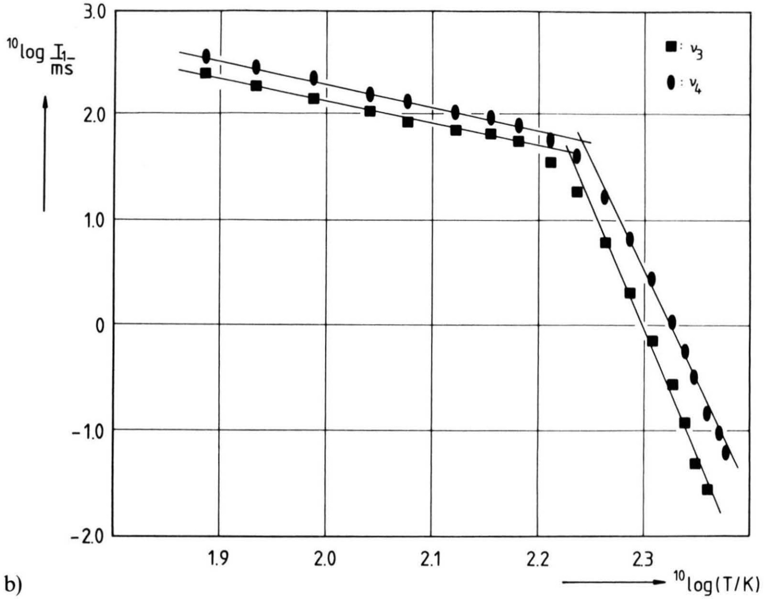

b)

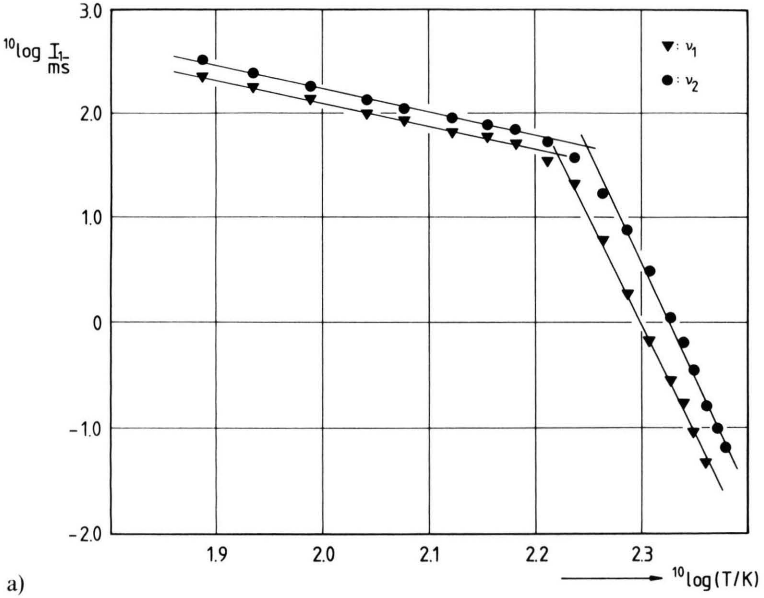

a)

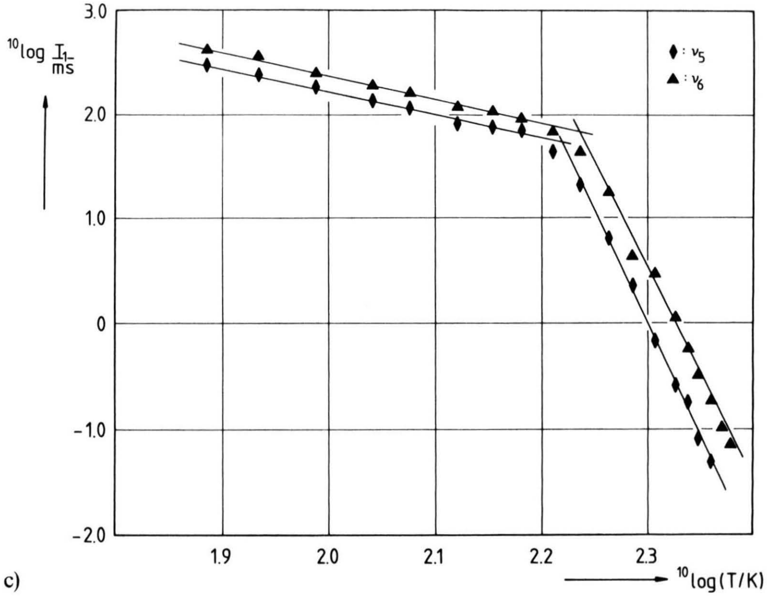

c)

Fig. 4. Logarithm of the ^{35}Cl spin-lattice relaxation time $T_1(^{35}\mathrm{Cl})$ of 1,2,3-$\mathrm{Cl_3D_3C_6}$ vs. the logarithm of temperature. a) $\mathrm{Cl}^{(\mathrm{I},1)}$: ▼; $\mathrm{Cl}^{(\mathrm{II},1)}$: ●; b) $\mathrm{Cl}^{(\mathrm{I},3)}$: ■; $\mathrm{Cl}^{(\mathrm{II},3)}$: ●; c) $\mathrm{Cl}^{(\mathrm{I},2)}$: ♦; $\mathrm{Cl}^{(\mathrm{II},2)}$: ▲.

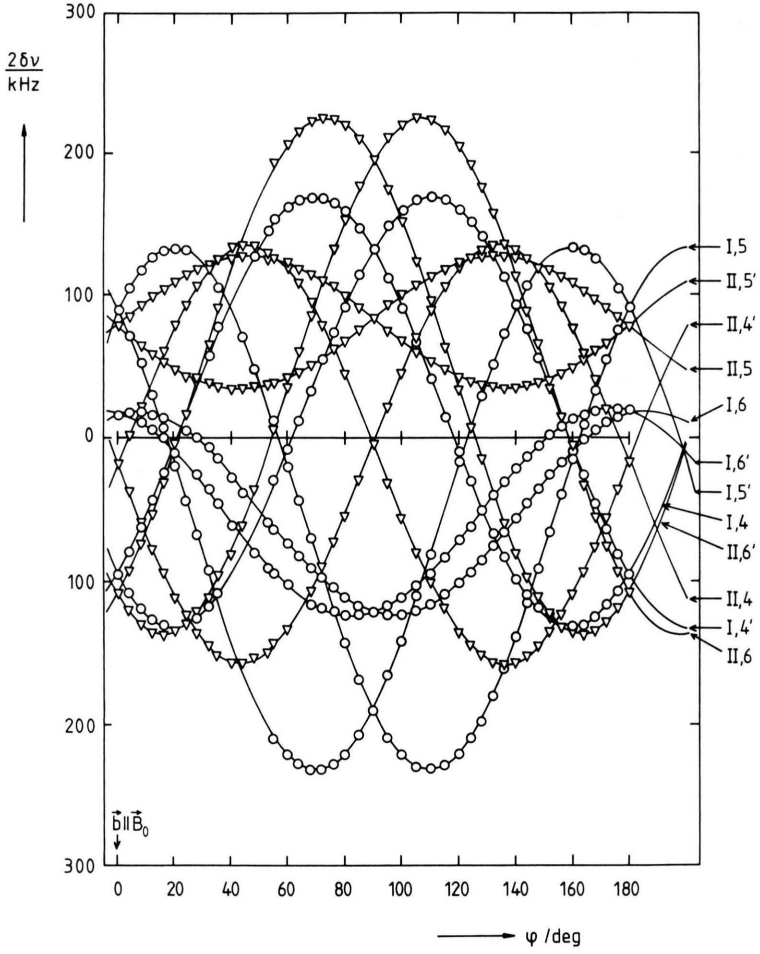

Fig. 5. Dependence of the quadrupole splitting $2\delta\nu$ of the ^{2}H NMR satellites of 1,2,3-$Cl_3D_3C_6$ on the orientation of the single crystal to the magnetic field $\boldsymbol{B}_0$. Twelve satellite pairs ($\nu_L+\delta\nu$, $\nu_L-\delta\nu$) are observed. The rotation axis of the crystal perpendicular to $\boldsymbol{B}_0$ is X [$\sphericalangle(\boldsymbol{a}, X) = \beta - 90°$]. The curves I,4; I,5; I,6; II,4; II,5 and II,6 belong to the corresponding atoms in Fig. 1, and all other curves to the symmetry related molecules. o: molecule I, ▿: molecule II. The mirror plane is located at $\varphi = 90°$; $\varphi = 0°$ for $\boldsymbol{b} \parallel \boldsymbol{B}_0$. $|B_0| = 4.7$ T; $\nu_L = 30.720$ MHz; $T = 295$ K.

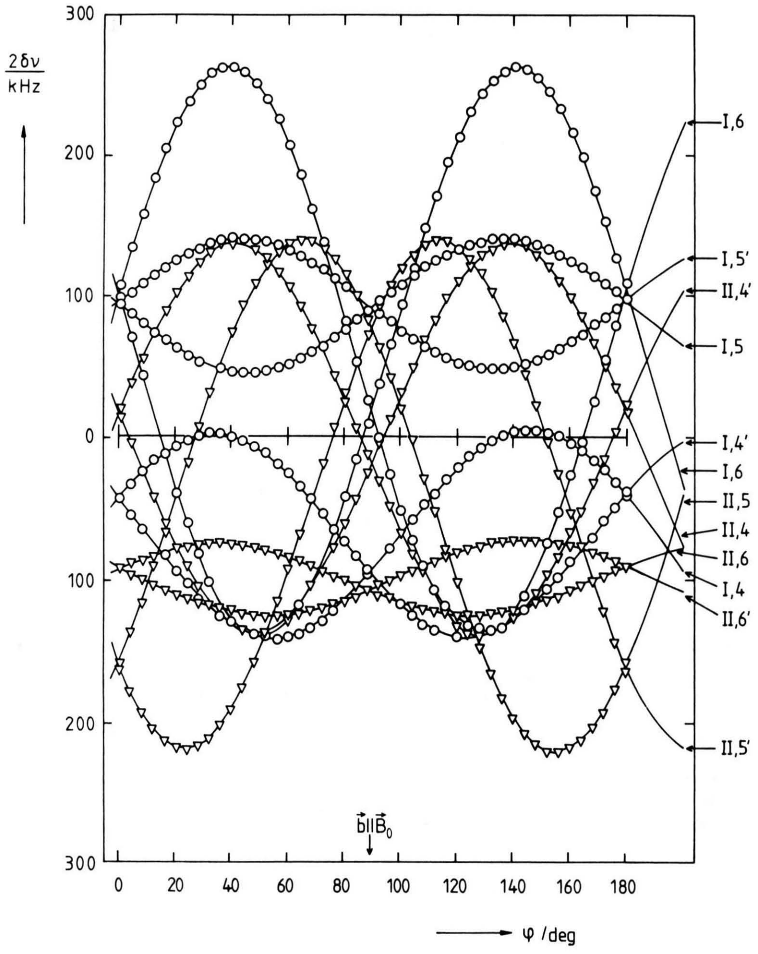

Fig. 6. Dependence of the quadrupole splitting $2\delta\nu$ of the ^{2}H NMR satellites of 1,2,3-$Cl_3D_3C_6$ on the orientation of the single crystal to the magnetic field $\boldsymbol{B}_0$. Twelve satellite pairs ($\nu_L+\delta\nu$, $\nu_L-\delta\nu$) are observed. The rotation axis of the crystal perpendicular to $\boldsymbol{B}_0$ is Z ($\boldsymbol{c} \parallel Z$). The curves I,4; I,5; I,6; II,4; II 5 and II 6 belong to the corresponding atoms in Fig. 1, while all other curves to the symmetry related molecules. o: molecule I, ▿: molecule II. The mirror plane is located at $\varphi = 0°$; $\varphi = 90°$ for $\boldsymbol{b} \parallel \boldsymbol{B}_0$. $|B_0| = 4.7$ T; $\nu_L = 30.720$ MHz; $T = 295$ K.

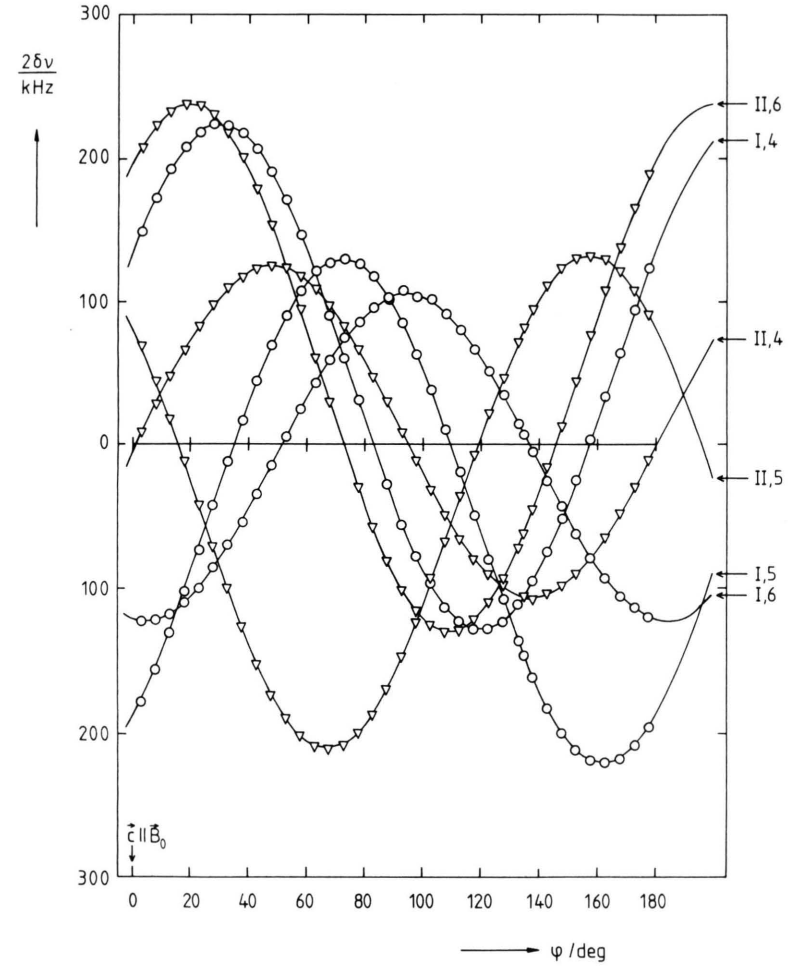

Fig. 7. Dependence of the quadrupole splitting $2\delta\nu$ of the ^{2}H NMR satellites of the 1,2,3-$Cl_3D_3C_6$ on the orientation of the single crystal to the magnetic field $\boldsymbol{B}_0$. Six satellite pairs ($\nu_L + \delta\nu$, $\nu_L - \delta\nu$) are observed. The rotation axis of the crystal perpendicular to $\boldsymbol{B}_0$ is Y($\boldsymbol{b} \parallel Y$). I,4; I,5; I,6; II,4; II,5 and II,6 are assigned to the corresponding atoms in Fig. 1. o: molecule I, ▿: molecule II. $\varphi = 0°$ for $\boldsymbol{c} \parallel \boldsymbol{B}_0$. $|B_0| = 4.7$ T; $\nu_L = 30.720$ MHz; $T = 295$ K.

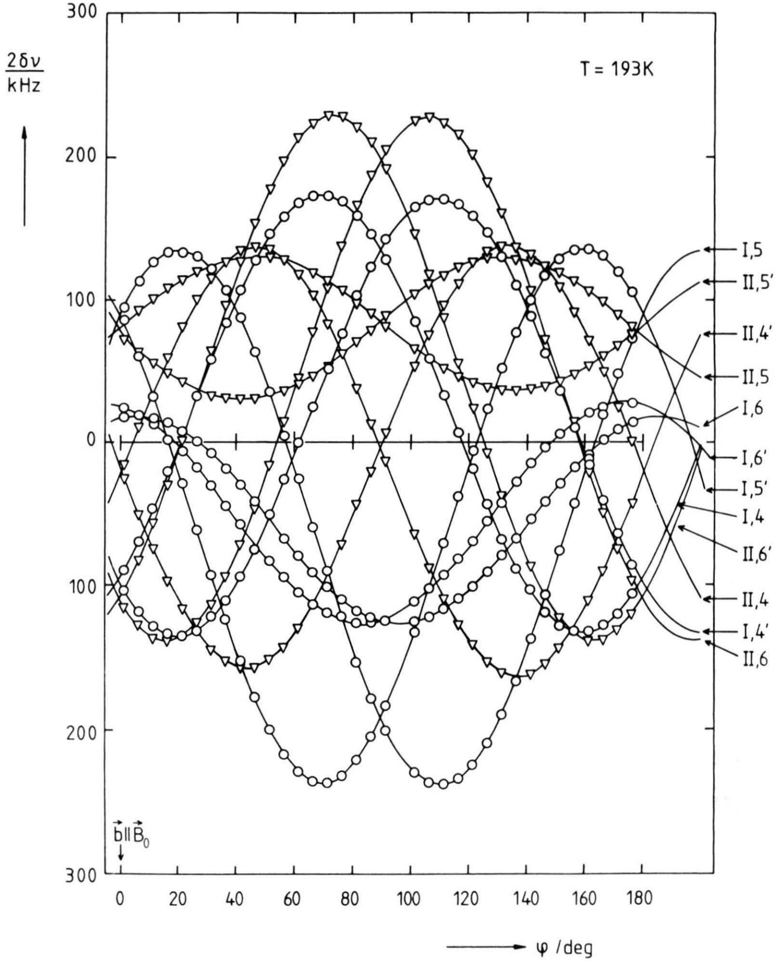

Fig. 8. Dependence of the quadrupole splitting $2\delta\nu$ of the ^{2}H NMR satellites of 1,2,3-$Cl_3D_3C_6$ on the orientation of the single crystal to the magnetic field $\boldsymbol{B}_0$. Twelve satellite pairs ($\nu_L + \delta\nu$, $\nu_L - \delta\nu$) are observed. The rotation axis of the crystal perpendicular to $\boldsymbol{B}_0$ is X [$\measuredangle(\boldsymbol{a}, X) = \beta - 90°$]. The curves I,4; I,5; I,6; II,4; II,5 and II,6 belong to the corresponding atoms in Fig. 1, all other curves to the symmetry related molecules. o: molecule I, ▿: molecule II. The mirror plane is located at $\varphi = 90°$; $\varphi = 0°$ for $\boldsymbol{b} \parallel \boldsymbol{B}_0$. $|B_0| = 4.7$ T; $\nu_L = 30.720$ MHz; $T = 193$ K.

Table 2. The quadrupolar splittings for rotation of the crystal around X, Y, Z $[\sphericalangle(\boldsymbol{a}, X)=\beta-90^\circ, \boldsymbol{b} \parallel Y, \boldsymbol{c} \parallel Z]$ are described by $2\delta\nu = A_i + B_i \cos(2\varphi) + C_i \sin(2\varphi)$; $i = X, Y, Z$. The resulting coefficients A_i, B_i and C_i, in units of kHz, are given for the ^{2}H EFG tensors of 1,2,3-$Cl_3D_3C_6$. $T = 295$ K.

$D^{(I,4)}$:	$A_X = 19.075$	$B_X = -113.929$	$C_X = 98.395$
	$A_Y = 47.686$	$B_Y = 86.855$	$C_Y = 153.752$
	$A_Z = -68.260$	$B_Z = 27.139$	$C_Z = -67.422$
$D^{(I,5)}$:	$A_X = 49.500$	$B_X = -140.866$	$C_X = 117.126$
	$A_Y = 45.881$	$B_Y = 143.639$	$C_Y = -101.429$
	$A_Z = -94.058$	$B_Z = -2.450$	$C_Z = 46.259$
$D^{(I,6)}$:	$A_X = 52.273$	$B_X = -69.851$	$C_X = -16.859$
	$A_Y = 52.273$	$B_Y = 113.086$	$C_Y = -16.859$
	$A_Z = -61.275$	$B_Z = -42.692$	$C_Z = -196.904$
$D^{(II,4)}$:	$A_X = -10.928$	$B_X = -6.756$	$C_X = -146.004$
	$A_Y = 8.991$	$B_Y = -11.889$	$C_Y = 115.171$
	$A_Z = 0.759$	$B_Z = 18.699$	$C_Z = -134.785$
$D^{(II,5)}$:	$A_X = -81.318$	$B_X = 2.714$	$C_X = 46.155$
	$A_Y = 39.254$	$B_Y = -122.327$	$C_Y = 121.234$
	$A_Z = 40.697$	$B_Z = 119.559$	$C_Z = -134.215$
$D^{(II,6)}$:	$A_X = 44.346$	$B_X = -151.773$	$C_X = -98.891$
	$A_Y = 53.910$	$B_Y = 143.709$	$C_Y = 115.653$
	$A_Z = -99.427$	$B_Z = 8.352$	$C_Z = 24.514$

Table 3. ^{2}H nuclear quadrupole coupling constants and asymmetry parameters η of 1,2,3-$Cl_3D_3C_6$ at 295 K. The e^2qQh^{-1} (^{2}H) is accurate to ±1 kHz, and η(^{2}H) to ±0.005.

Atom	e^2qQh^{-1}/kHz	η
$D^{(I,4)}$	175.8	0.066
$D^{(I,5)}$	177.2	0.065
$D^{(I,6)}$	176.1	0.066
$D^{(II,4)}$	177.3	0.064
$D^{(II,5)}$	179.5	0.060
$D^{(II,6)}$	177.2	0.073

Table 4. Direction cosines of the principal axes Φ_{ii} $(i = x, y, z)$ of the ^{2}H electric field gradient tensors and of the corresponding bond directions $C^{(j)}-D^{(j)}$ $(j = 4, 5, 6)$ in the orthogonal axes system X, Y, Z $[\sphericalangle(\boldsymbol{a}, X)=\beta-90^\circ, \boldsymbol{b} \parallel Y, \boldsymbol{c} \parallel Z]$ in crystalline 1,2,3-$Cl_3D_3C_6$. For the numbering of the atoms, see Figure 1. The direction cosines are defined as $\lambda_i = \cos(\Phi_{ii}, X)$, $\mu_i = \cos(\Phi_{ii}, Y)$ and $\nu_i = \cos(\Phi_{ii}, Z)$. $T = 295$ K.

	λ_i	μ_i	ν_i
$\Phi_{xx}(D^{(I,4)})$	−0.60571	0.55296	0.57217
$\Phi_{yy}(D^{(I,4)})$	0.63157	0.77149	−0.07699
$\Phi_{zz}(D^{(I,4)})$	−0.48400	0.31473	−0.81651
$C^{(I,4)}-D^{(I,4)}$	−0.48986	0.31512	−0.81286
$\Phi_{xx}(D^{(I,5)})$	−0.71850	0.54263	−0.43510
$\Phi_{yy}(D^{(I,5)})$	0.63103	0.77165	−0.07972
$\Phi_{zz}(D^{(I,5)})$	0.29247	−0.33184	−0.89685
$C^{(I,5)}-D^{(I,5)}$	0.28025	−0.33385	−0.90001
$\Phi_{xx}(D^{(I,6)})$	−0.14041	−0.07775	−0.98707
$\Phi_{yy}(D^{(I,6)})$	0.61345	0.77566	−0.14837
$\Phi_{zz}(D^{(I,6)})$	0.77714	−0.62634	−0.06121
$C^{(I,6)}-D^{(I,6)}$	0.77558	−0.62793	−0.06458
$\Phi_{xx}(D^{(II,4)})$	0.69360	0.07776	0.71615
$\Phi_{yy}(D^{(II,4)})$	0.49253	−0.77664	−0.39271
$\Phi_{zz}(D^{(II,4)})$	0.52565	0.62512	−0.57698
$C^{(II,4)}-D^{(II,4)}$	0.51993	0.62274	−0.58469
$\Phi_{xx}(D^{(II,5)})$	0.07483	0.57520	−0.81459
$\Phi_{yy}(D^{(II,5)})$	−0.50608	0.72577	0.46599
$\Phi_{zz}(D^{(II,5)})$	0.85924	0.37738	0.34540
$C^{(II,5)}-D^{(II,5)}$	0.85731	0.37701	0.35054
$\Phi_{xx}(D^{(II,6)})$	0.79702	0.59495	−0.10395
$\Phi_{yy}(D^{(II,6)})$	−0.51549	0.75981	0.39618
$\Phi_{zz}(D^{(II,6)})$	0.31469	−0.26217	0.91226
$C^{(II,6)}-D^{(II,6)}$	0.31706	−0.25822	0.91257

Discussion

The results of the temperature dependence measurements of the ^{35}Cl NQR frequencies, the linewidths and the spin-lattice relaxation times $T_1(^{35}Cl)$ for deuterated 1,2,3-trichlorobenzene are the same as those reported for 1,2,3-$Cl_3H_3C_6$ [6]. The signals die out in the range of $240 \leqq T/K \leqq 260$. The ^{35}Cl NQR frequencies of molecule I (ν_1, ν_3, ν_5) disappear at lower temperatures than those of molecule II (ν_2, ν_4, ν_6). With equation

$$\Delta\nu = c \cdot \exp(-E_A/RT), \tag{4}$$

from the plot $\log \Delta\nu = f(1/T)$, see Fig. 10, an activation energy E_A for the bleaching out process was calculated. The values are listed in Table 7, in which the data for the protonated compound are given for comparison, too. Additionally, E_A obtained from temperature dependence measurements of $T_1(^{35}Cl)$ are given,

$$1/T_1 = c' \cdot \exp(-E_A/RT). \tag{5}$$

Within the limits of error, the values are the same for the protonated and the deuterated trichlorobenzene. For $\nu_2(^{35}Cl)$ and $\nu_3(^{35}Cl)$, the activation energies were slightly higher than those obtaind for the other frequencies, 40.1 and 42.3 kJ mol^{-1}, respectively. These two frequencies are close together (see Fig. 2) and additional relaxation processes may occur. Therefore the mean values for E_A from the $T_1(^{35}Cl)$ measurements, given in Table 7, were calculated neglecting ν_2 and ν_3. Before the bleaching out process sets in, librations are the main contribution to the spin-lattice relaxation time. According to (6), we find exponents n in the range of $2.1 \leqq n \leqq 2.4$,

$$1/T_1 = a \cdot T^n. \tag{6}$$

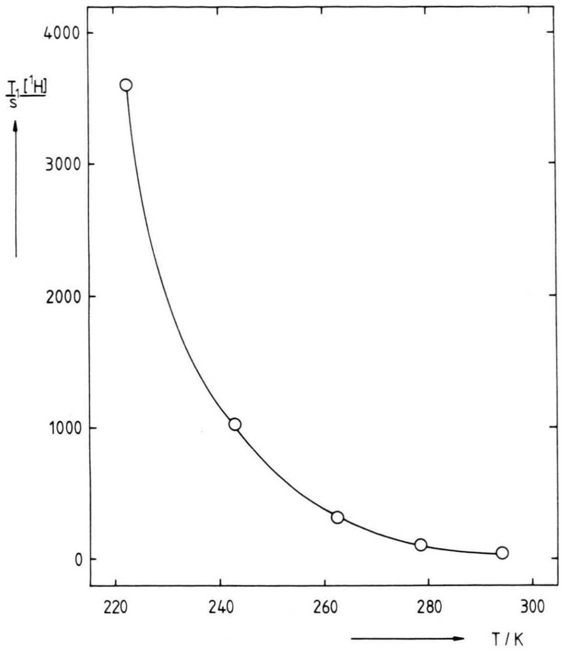

Fig. 9. Temperature dependence of the spin-lattice relaxation time T_1 of the protons of polycrystalline 1,2,3-$Cl_3H_3C_6$. $|B_0| = 4.7$ T.

In the case of librational motions this exponent has the theoretical value 2 [19, 20].

With the results of the ^{35}Cl NQR measurements, the model of formation and migration of lattice vacancies and order-disorder transitions can be excluded. Distortion of the crystal lattice would have a similar influence on the molecules I and II. The NQR results, however, show that the signals of molecules I begin to broaden at lower temperature than those of molecules II. Furthermore, also the protons are involved in the process. For both Cl and H the same E_A-values from T_1 measurements were found. This result is also in disagreement with a lattice vacancies model. An other mechanism therefore must be responsible for the bleaching out.

A possible mechanism is the reorientational motion of the molecules. To get further informations we investigated the temperature dependence of $T_1(^1H)$ in 1,2,3-$Cl_3H_3C_6$ (see Figure 9). Evaluation of the data according the BPP (Bloembergen, Purcell, Pound) theory [21], with the condition

$$\omega \cdot \tau_c \gg 1, \tag{7}$$

(τ_c is the correlation time of the reorientational motion) leads to $E_A = 35.1$ kJ mol^{-1}.

Table 5. Angles between the principal axes of the ^{2}H electric field gradient tensors and structure elements of the molecule 1,2,3-$Cl_3D_3C_6$ in the solid state. $\boldsymbol{n}_{R\,I}$ is the normal to the ring plane of molecule I, $\boldsymbol{n}_{R\,II}$ is the normal to the ring plane of molecule II. $j = 4, 5, 6$; $T = 295$ K.

Molecule I

Angle	$D^{(I,4)}$	$D^{(I,5)}$	$D^{(I,6)}$
$\sphericalangle(\Phi_{zz}^{(j)}, C^{(j)}-D^{(j)})$	0.4°	0.7°	0.3°
$\sphericalangle(\Phi_{xx}^{(j)}, \boldsymbol{n}_{R\,I})$	90.2°	89.7°	93.4°
$\sphericalangle(\Phi_{yy}^{(j)}, \boldsymbol{n}_{R\,I})$	0.6°	0.5°	3.6°
$\sphericalangle(\Phi_{zz}^{(j)}, \boldsymbol{n}_{R\,I})$	89.4°	89.7°	89.5°
$\sphericalangle(C^{(j)}-D^{(j)}, \boldsymbol{n}_{R\,I})$	89.6°	90.2°	89.6°

Molecule II

Angle	$D^{(II,4)}$	$D^{(II,5)}$	$D^{(II,6)}$
$\sphericalangle(\Phi_{zz}^{(j)}, C^{(j)}-D^{(j)})$	0.6°	0.3°	0.4°
$\sphericalangle(\Phi_{xx}^{(j)}, \boldsymbol{n}_{R\,II})$	90.0°	85.3	88.8°
$\sphericalangle(\Phi_{yy}^{(j)}, \boldsymbol{n}_{R\,II})$	−0.6°	4.7°	1.3°
$\sphericalangle(\Phi_{zz}^{(j)}, \boldsymbol{n}_{R\,II})$	90.5°	89.9°	89.7°
$\sphericalangle(C^{(j)}-D^{(j)}, \boldsymbol{n}_{R\,II})$	90.6°	89.7°	89.6°

Table 6. The quadrupolar splittings for rotation of the crystal around X [$\sphericalangle(\boldsymbol{a}, X = \beta - 90°$] are described by $2\delta\nu = A_X + B_X \cos(2\varphi) + C_X \sin(2\varphi)$. The resulting coefficients A_X, B_X and C_X are given for the ^{2}H EFG tensors of 1,2,3-$Cl_3D_3C_6$. $T = 193$ K.

$D^{(I,4)}$:	$A_X = 19.042$	$B_X = -116.113$	$C_X = 100.560$
$D^{(I,5)}$:	$A_X = 50.825$	$B_X = -141.976$	$C_X = 121.713$
$D^{(I,6)}$:	$A_X = 52.017$	$B_X = -\ 73.488$	$C_X = -\ 16.797$
$D^{(II,4)}$:	$A_X = -11.886$	$B_X = -\ 8.441$	$C_X = -148.831$
$D^{(II,5)}$:	$A_X = -82.000$	$B_X = 3.342$	$C_X = 48.273$
$D^{(II,6)}$:	$A_X = 44.733$	$B_X = -154.282$	$C_X = -\ 99.680$

Table 7. Values of the activation energies E_A for the bleaching out process, obtained from temperature dependence measurements of the linewidth of the ^{35}Cl NQR signals, spin-lattice relaxation time $T_1(^{35}Cl)$ and $T_1(^1H)$ for 1,2,3-trichlorobenzene and the deuterated compound.

Measurement	1,2,3-$Cl_3H_3C_3$ E_A/kJ · mol^{-1}	1,2,3-$Cl_3D_3C_6$ E_A/kJ · mol^{-1}
$\Delta\nu = f(T)$ molecule I	30.6 [6]	32.2
molecule II	35.6 [6]	36.4
$T_1(^{35}Cl) = f(T)$	39.0 [6]	38.3
$T_1(^1H) = f(T)$	35.1	–

This value agrees with the results of the ^{35}Cl NQR measurements (see Table 7). Both chlorine and hydrogen are involved in the activated process. For that reason ^{2}H NMR measurements with deuterated 1,2,3-trichlorobenzene should yield additional information about the bleaching out process.

In contrast to ^{1}H, the deuteron nucleus possesses a quadrupole moment, eQ, and therefore the EFG's at

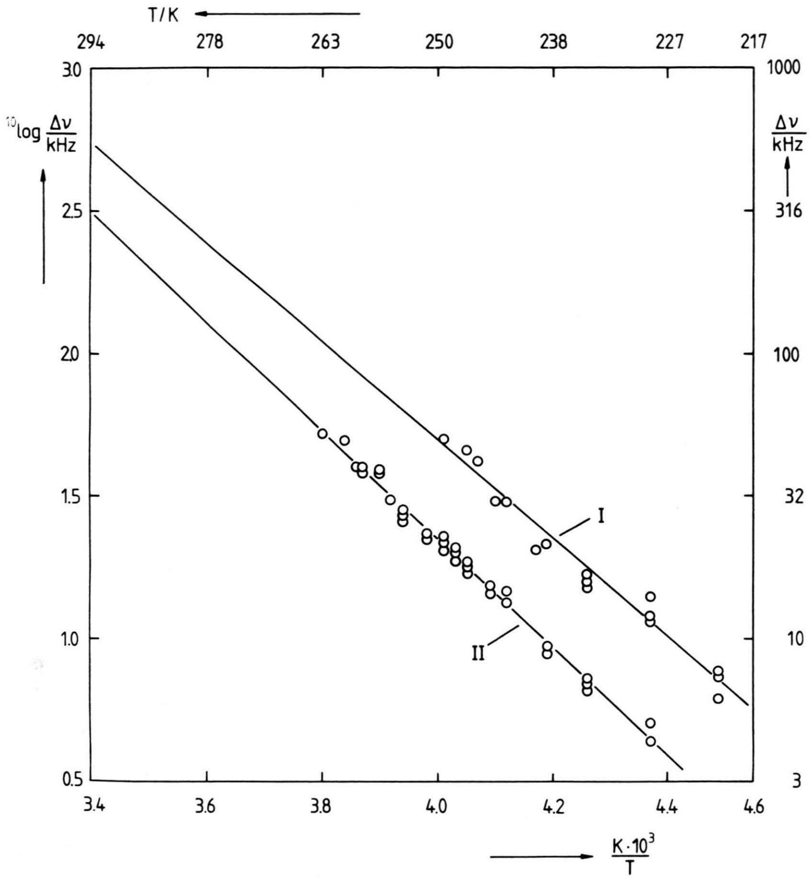

Fig. 10. Logarithm of the linewidths of the ^{35}Cl NQR signals of 1,2,3-$Cl_3D_3C_6$. The values are extrapolated to room temperature.

this site can be studied. Since $eQ(^2H)$ is quite small ($2.8 \cdot 10^{-3}$ barn), a low quadrupole interaction results. ^{2}H NQR frequencies are directly not easily to detect. $e^2qQh^{-1}(^2H)$ and $\eta(^2H)$ may be determined by double resonance techniques [22] with polycrystalline sample. In case one wishes to know the orientation of the principal axes $\Phi_{xx}(^2H)$, $\Phi_{yy}(^2H)$ and $\Phi_{zz}(^2H)$ of the EFGT with respect to the molecule, high field single crystal ^{2}H NMR must be applied [23].

The NQCC's of D in 1,2,3-$Cl_3D_3C_6$ at room temperature are in the range of $175.8 \leqq e^2qQh^{-1}(^2H)/\mathrm{kHz} \leqq 179.5$ (see Table 3). These values are smaller than those for other chlorobenzenes (see Table 8, in which some data taken from the literature are listed). The results for 1,2,3-$Cl_3D_3C_6$, however, can not directly be compared with the values given in Table 8 because they were obtained at different temperatures. The $e^2qQh^{-1}(^2H)$ values of 1,2,3-$Cl_3D_3C_6$ were determined at 295 K, whereas the compounds in Table 8 (except anthracene) were investigated at 77 K. Let us therefore estimate the values of $e^2qQh^{-1}(^2H)$ for 1,2,3-$Cl_3D_3C_6$ at 77 K. Librational motions, which increase with increasing temperature, lead to a decrease of the NQCC at the chlorine site of chlorobenzenes. For aliphatic compounds like CD_2Cl_2 and $CDCl_3$, such a temperature dependence for e^2qQh^{-1} of the deuteron has been observed, too [18]. The same should be valid for e^2qQh^{-1} of D bound to the aromatic ring.

From 77 to 250 K, the ^{35}Cl NQR frequencies change by about 500 kHz (see Figure 2). This corresponds to a change in $e^2qQh^{-1}(^{35}Cl)$ of ≈ 1 MHz. These changes are in the order of 1.5%. Since the librational motions should have a similar influence on Cl and D, a change of $e^2qQh^{-1}(^2H)$ of about 1.8% can be expected, going from room temperature to 77 K. $e^2qQh^{-1}(^2H)$ of 1,2,3-$Cl_3D_3C_6$ at room temperature has a mean value of 177 kHz. For 77 K, values of ≈ 180 kHz can be expected, which are in the same order of magnitude as $e^2qQh^{-1}(^2H)$ of 1,2,3-$Cl_4D_2C_6$ (see Table 8).

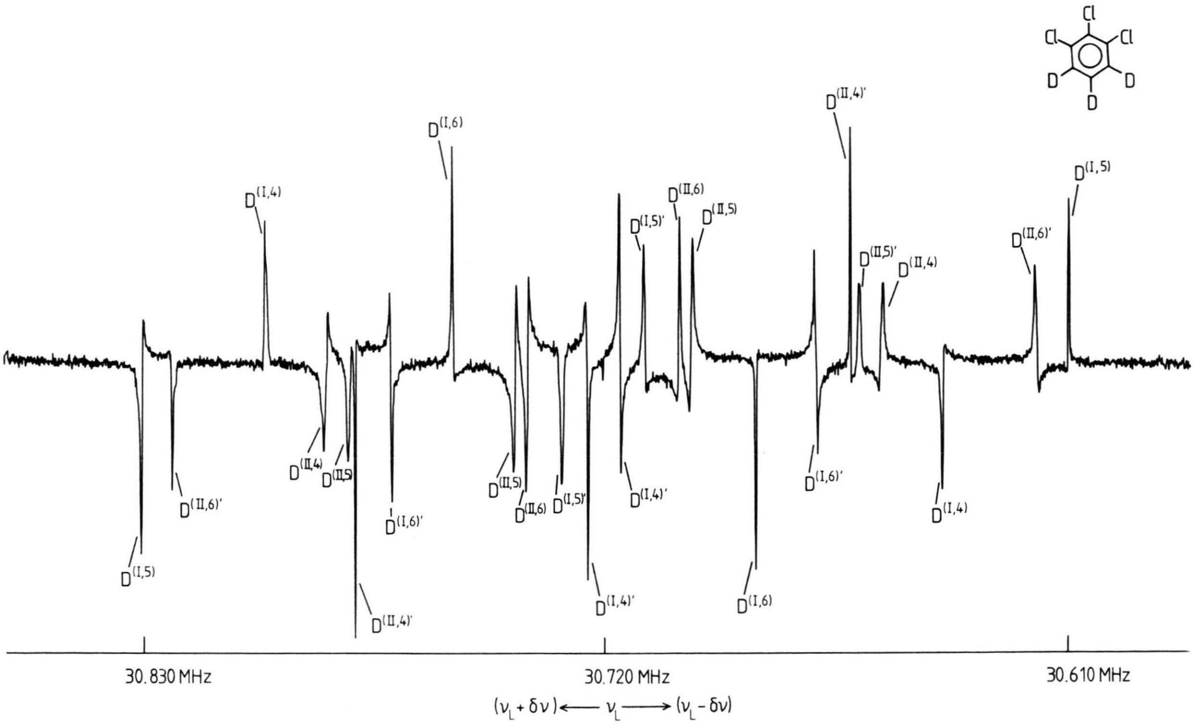

Fig. 11. Typical ^{2}H NMR spectrum of a single crystal of 1,2,3-$Cl_3D_3C_6$ at room temperature.

Table 8. $e^2qQh^{-1}(^2H)$ and $\eta(^2H)$ of some aromatic compounds at $T = 77$ K. The $e^2qQh^{-1}(^2H)$ and $\eta(^2H)$ of anthracene were determined at room temperature by single crystal ^{2}H NMR.

Compound	$e^2qQh^{-1}(^2H)$/ kHz	$\eta(^2H)$	Ref.
Benzene	180.7 ± 1.5	0.041 ± 0.007	[24]
Toluene	179.9 ± 1.7	0.056 ± 0.002	[24]
Ethylbenzene	177.8 ± 2.2	0.063 ± 0.003	[24]
Naphtalene	176.7 ± 1.5	0.053 ± 0.005	[24]
1,4-Dichloro-benzene	183.3	0.059	[25]
1,3,5-Trichloro-benzene	181.9 ± 0.3	$\approx 0.06-0.08$	[26]
1,2,3,4-Tetra-chlorobenzene	180.7 ± 0.2	0.065	[26]
Anthracene (3 independent ^{2}H EFGT's in the unit cell)			
$178.0 \leqq e^2qQh^{-1}(^2H)/\mathrm{kHz} \leqq 184.0$			[23]
$0.051 \leqq \eta(^2H) \leqq 0.076$			

The η values of 1,2,3-$Cl_3D_3C_6$ range from 0.060 to 0.073. These are typical values for D bound to the aromatic ring (see Table 8). Whereas a non axial EFG at the chlorine site in chlorobenzenes can be explained by the double bond character of the C–Cl bond [27], this explanation does not hold for D. The deuteron possesses a 1s-electron. The probability for occupation of the first non-occupied p-orbital is very low since it lies energetically high. Double bonding therefore is not possible. The non-axial EFG's at the deuteron site in deuterobenzenes have to be explained by the asymmetric surroundings of the carbon atom (sp^2-carbon) to which D is bound.

For the orientation of the principal axes of the EFG's at the deuteron sites in 1,2,3-$Cl_3D_3C_6$ it was found that $\Phi_{zz}(^2H)$ is parallel to the C–D bond, $\Phi_{yy}(^2H)$ is perpendicular to the benzene ring plane and $\Phi_{xx}(^2H)$ lies in the ring plane. The deviations from this ideal orientation, which also was observed in anthracene [23], are small (see Table 5).

A typical ^{2}H NMR spectrum at 295 K is shown in Figure 11. The satellites are intense and the lines are narrow (see Figure 12). Temperature dependence measurements between $193 \leqq T/\mathrm{K} \leqq 295$ of the spectrum at constant orientation of the crystal to the magnetic field $\boldsymbol{B}_0$ revealed that the linewidths of the satellites do not depend on temperature.

To find out whether the orientation of $\Phi_{zz}(^2H)$ with respect to the crystal changes at temperatures below the bleaching out point, rotation of the crystal around X [$\sphericalangle(\boldsymbol{a}, X) = \beta - 90^\circ$] at $T = 193$ K was carried out.

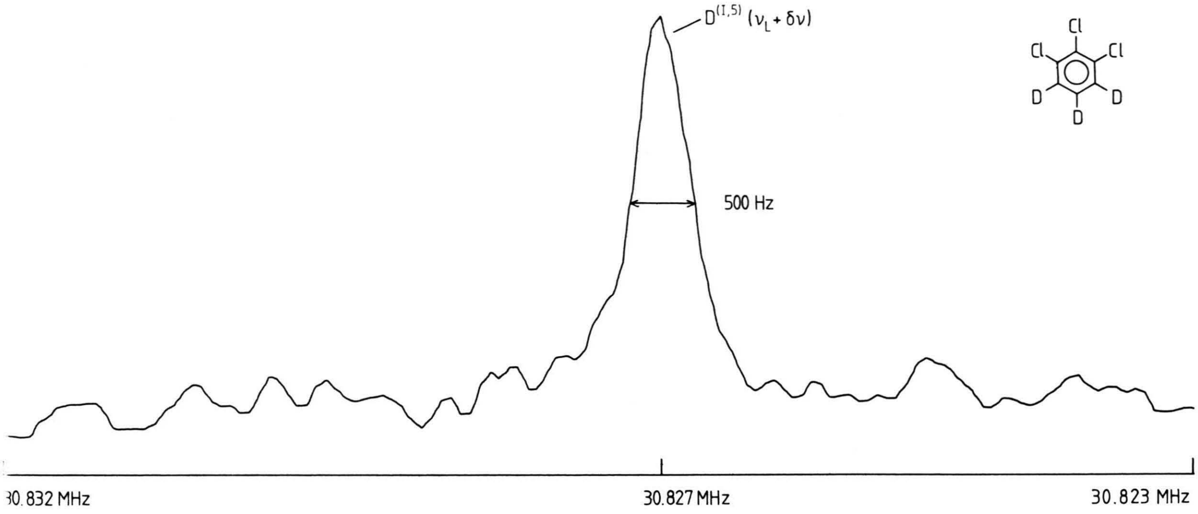

Fig. 12. Linewidth of a ^{2}H NMR satellite of 1,2,3-$Cl_3D_3C_6$ at room temperature.

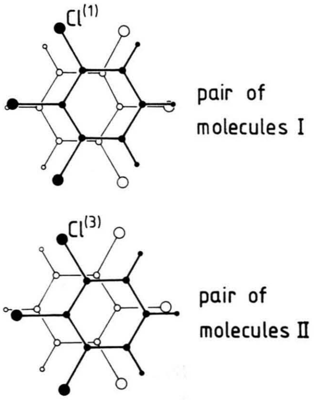

Fig. 13. Antiparallel arrangement of the pairs of dipole molecules in crystalline 1,2,3-trichlorobenzene.

The result is shown in Figure 8. Nearly identical rotation patterns are obtained for 193 K and 295 K (compare Figs. 8 and 5). This is also evident from the coefficients A_X, B_X and C_X which describe the curves (see Tables 6 and 2). The small differences may be due to temperature dependence of $e^2 q Q h^{-1}$ (^{2}H) discussed above. Single crystal measurements are tedious. For the reason we didn't rotate the crystal at 193 K around two further axes to determine $e^2 q Q h^{-1}$ (^{2}H) and η(^{2}H) exactly. Those results wouldn't contribute to the interpretation of the bleaching out phenomenon anyway.

The main result we get from the ^{2}H NMR experiments is an information about the time scale of the reorientation. This motion, which leads to a broadening of the ^{35}Cl NQR signals of about 300–500 kHz at room temperature (extrapolated from Fig. 10), has no measurable influence on the ^{2}H NMR satellites. The linewidth of the ^{2}H NMR satellites is about 500 Hz (see Fig. 12) and independent of temperature. So the contribution of the reorientational motion to $\delta\nu$ can not exceed 500 Hz. At room temperature values for "static molecules" for the coupling constants, asymmetry parameters and direction cosines of th EFGT's of the ^{2}H atoms have been obtained. Thus the condition $\omega_Q \cdot \tau_c \gg 1$ is fulfilled, and according to

$$\tau_c = 1/2\pi\,\Delta\nu \tag{8}$$

the correlation time τ_c for the reorientational motion has to be in the order of milliseconds at room temperature. Since τ_c is temperature dependent [28],

$$\tau_c = \tau_0 \cdot \exp(E_A/RT)\,, \tag{9}$$

the reorientation rate near the bleaching out temperature should be even much smaller.

To illustrate the reorientation mechanism, let us have a look at the crystal structure again. The molecules are arranged in centrosymmetric units, each pair consisting of one sort of molecules I or II (see Figure 13). The distance between the benzene ring planes of the molecules forming a pair of dipoles is 352.8 pm and 353.2 pm for molecules I and II, respectively (compare Fig. 14, in which a projection of a part of the structure onto the ***a***, ***b*** plane is shown). Since E_A for the process is relatively small, reorientational motion of a pair of dipoles can be assumed. Reorientation of a single molecule of a pair would destroy the anti-

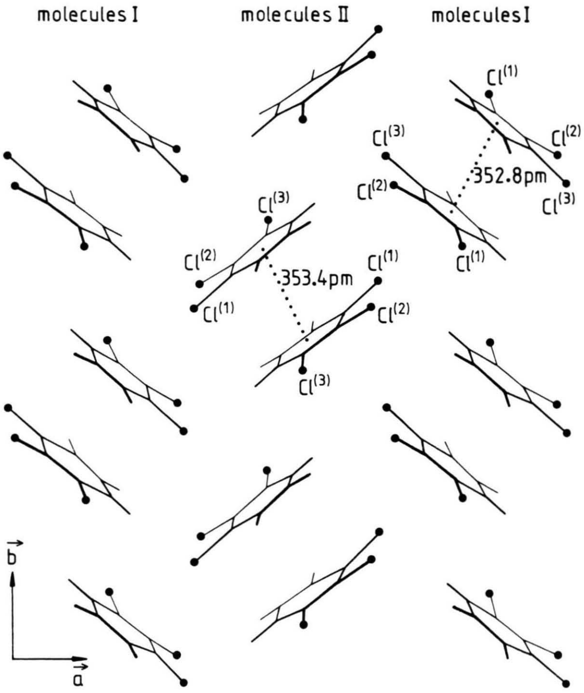

Fig. 14. Projection of a part of the crystal structure of 1,2,3-trichlorobenzene onto the ***a***, ***b*** plane.

parallel arrangement of the dipoles, further the bulky Cl atoms of the two molecules would come close together, and a higher E_A should result. We propose that the molecules rotate about an axis shown in Figure 15. That there is enough space for such a motion can be seen in Figure 14.

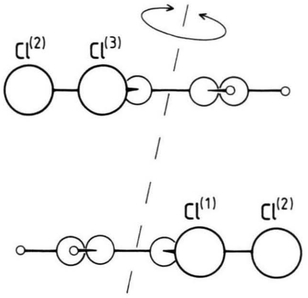

Fig. 15. Projection of a pair of 1,2,3-trichlorobenzene molecules along the ring plane. Also the reorientation axis is sketched.

Near the bleaching out temperature, the reorientation rate is low, approximately in the time scale of seconds. Molecules of type II begin to rotate at ≈20 K higher. With increasing temperature the reorientation rate increases and contributes to the T_1 mechanism of the Cl and H atoms. The dynamic process in the lattice leads to a broadening of the ^{35}Cl NQR signals. This broadening is not an effect of a fluctuating EFG produced by a distorted lattice but is due to a relaxation path caused by reorientational motion. This T_1 mechanism has a dominating influence on the linewidth of the Cl signals [28]. The reorientation rate at room temperature is surprisingly low in comparison to the T_1 data of the Cl atoms and is in the order of milliseconds as derived from the ^{2}H NMR spectra.

We are grateful to the Deutsche Forschungsgemeinschaft and to the Fonds der Chemischen Industrie for support of this work.

[1] Al. Weiss, J. Mol. Struct. **83,** 181 (1982).
[2] W. Pies and Al. Weiss, Z. Phys. Chem. N.F. **127,** 147 (1981).
[3] C. A. Martin and M. J. Zuriaga, Z. Naturforsch. **41 a,** 378 (1986).
[4] I. Tatsuzaki, J. Phys. Soc. Japan **14,** 578 (1959).
[5] W. Pies, Dissertation, D 17, Darmstadt 1978.
[6] S. Sharma, N. Weiden, and Al. Weiss, Ber. Bunsenges. Phys. Chem. **90,** 725 (1986).
[7] R. G. Hazell, M. S. Lehmann, and G. S. Pawley, Acta Cryst. **B 28,** 1388 (1972).
[8] P. J. Bray and R. G. Barnes, J. Chem. Phys. **27,** 551 (1957).
[9] E. I. Fedin, Zh. Strukt. Khim. **1,** 124 (1960).
[10] A. H. White, B. S. Biggs, and S. O. Morgan, J. Amer. Chem. Soc. **62,** 16 (1960).
[11] N. H. Werstiuk and T. Kadai, Can. J. Chem. **51,** 1485 (1973).
[12] N. H. Werstiuk and T. Kadai, Can. J. Chem., **52,** 2169 (1974).
[13] G. Fischer and P. Puza, Synthesis **1973,** p. 218.
[14] G. M. Volkoff, H. E. Petch, and D. W. L. Smellie, Can. J. Phys. **30,** 270 (1952).
[15] G. M. Volkoff, Can. J. Phys. **31,** 820 (1953).
[16] G. Hutton and B. Pedersen, J. Magn. Res. **13,** 119 (1974).
[17] R. G. Barnes, Adv. in NQR, J. A. S. Smith, Edt. 1974, p. 1.
[18] J. L. Ragle, M. Mokarram, D. Presz, and G. Minott, J. Magn. Res. **20,** 195 (1975).
[19] D. E. Woessner and H. S. Gutowsky, J. Chem. Phys. **39,** 440 (1963).
[20] J. van Kranendonk and M. B. Walker, Can. J. Phys. **46,** 2441 (1986).
[21] N. Bloembergen, E. M. Purcell, and R. V. Pound, Phys. Rev. **73,** 679 (1948).
[22] M. E. Emshwiller, E. L. Hahn, and D. Kaplan, Phys. Rev. **118,** 414 (1960).
[23] D. M. Ellis and J. L. Bjorkstam, J. Chem. Phys. **46,** 4460 (1967).
[24] R. G. Barnes and J. W. Bloom, J. Chem. Phys. **57,** 3082 (1972).
[25] M. Schwab and E. L. Hahn, J. Chem. Phys. **52,** 3158 (1970).
[26] J. L. Ragle and M. Mokarram, J. Chem. Phys. **62,** 3361 (1975).
[27] R. Bersohn, J. Chem. Phys. **22,** 2078 (1954).
[28] H. Chihara and N. Nakamura, Adv. in NQR, J. A. S. Smith, Edt. 1980, p. 4.